

## Direct Observation of a $\beta$ -SiC(100)- $c(4 \times 2)$ Surface Reconstruction

P. Soukiassian,<sup>1</sup> F. Semond,<sup>1</sup> L. Douillard,<sup>1</sup> A. Mayne,<sup>2</sup> G. Dujardin,<sup>2</sup> L. Pizzagalli,<sup>3</sup> and C. Joachim<sup>3</sup>

<sup>1</sup>*Commissariat à l'Énergie Atomique, DSM-DRECAM-SRSIM, Bâtiment 462,*

*Centre d'Études de Saclay, 91191 Gif sur Yvette Cedex*

*and Département de Physique, Université de Paris-Sud, 91405 Orsay Cedex, France*

<sup>2</sup>*Laboratoire de Photophysique Moléculaire, Bâtiment 213, Université de Paris-Sud, 91405 Orsay Cedex, France*

<sup>3</sup>*Centre d'Elaboration de Matériaux et d'Études Structurales, UPR 8011 B.P. 4347,31055 Toulouse Cedex 4, France*

(Received 5 August 1996)

We provide the first direct observation of a  $\beta$ -SiC(100)- $c(4 \times 2)$  surface reconstruction. The experiments are performed using high-resolution scanning tunneling microscopy (STM). Flat surfaces having a long range order are grown. Individual Si dimers are identified and form a centered pseudohexagonal pattern give a  $c(4 \times 2)$  array. Further support for Si-dimer identification is provided by theoretical STM image calculations. The results suggest a model of dimer rows having alternatively up and down dimers (AUDD) within the row, in an "undulating" type of arrangement reducing the surface stress. Hence the  $\beta$ -SiC(100)- and Si(100)- $c(4 \times 2)$  surface reconstructions are very different. [S0031-9007(96)02270-3]

PACS numbers: 68.35.Bs, 81.65.-b

Cubic ( $\beta$ ) silicon carbide (SiC), especially its (100) face, is expected to have a similar surface structure to those of elemental semiconductors (Si, Ge). However, unlike Si (Ge),  $\beta$ -SiC is not a covalent semiconductor and, due to an underlying C layer, its (100) face is a polar surface. Therefore the understanding of  $\beta$ -SiC(100) surface is of major interest, while it is challenging to compare similar surfaces having non-polar-Si(100) or polar- $\beta$ -SiC(100) characters. In addition, due to the very large mismatch between Si and  $\beta$ -SiC lattice parameters [1,2], Si atoms are "compressed" by  $\approx 20\%$  on a Si-terminated  $\beta$ -SiC(100) surface. This very special situation cannot be reproduced on Si surfaces. In this view, the  $\beta$ -SiC(100) is also a prototypical case especially suitable to study surface stress effects. SiC is an advanced large band-gap IV-IV compound and refractory semiconductor with hexagonal ( $\alpha$ ) and cubic ( $\beta$ ) phases [1,2]. Because of a unique combination of exceptional properties, SiC is expected, within the next decade, to challenge silicon in high temperature, high speed, high power, and high voltage sensor and electronic devices [1]. Furthermore, SiC is one of the best biocompatible materials, especially with blood, while very interesting mechanical properties makes this ceramic suitable for matrix composites. These major technological interests are driving forces behind the present rapid growth of fundamental investigations of SiC surfaces [2-9].

It was recently shown that SiC interface formation very much depends on the surface reconstruction [8]. SiC surface structure knowledge, which is far from that of other semiconductors (Si, Ge or III-V), is a key issue to get deep insights and control of  $\beta$ -SiC(100) surfaces/interfaces. Depending on the surface composition (Si/C ratio), several reconstructions have been observed by low energy electron diffraction (LEED) [2-9]. The observation of  $2 \times 1$  LEED patterns has induced a strong basic interest for the  $\beta$ -SiC(100) surface, due to the expected analogy with

Si(100) [2,7]. The existence of another reconstruction having the same Si/C ratio, the  $c(4 \times 2)$ , has also been proposed [2,4,5]. While the  $2 \times 1$  surface reconstruction existence is believed to be well established, this is not the case for the  $c(4 \times 2)$  one, with a few reports only [2,4,5]. Actually, the  $\beta$ -SiC(100)- $c(4 \times 2)$  reconstruction remains rather difficult to evidence, probably inhibited by surface roughness or contamination as pointed out [2]. The  $2 \times 1$  and  $c(4 \times 2)$  reconstructions represent models of an ideally Si-terminated  $\beta$ -SiC(100) surface [2]. So far, studies of  $\beta$ -SiC(100) $2 \times 1$  and  $c(4 \times 2)$  structures were based on nonreal space probes, with no scanning tunneling microscopy (STM) study.

In this Letter, we investigate the Si-terminated  $\beta$ -SiC(100) surface by high resolution STM. We provide the first direct observation of a  $\beta$ -SiC(100)- $c(4 \times 2)$  surface reconstruction. The experimental data, together with STM image calculations, suggest a model of Si-Si dimer rows having alternatively up and down dimers (AUDD) leading to reduced surface stress. Contrary to previous belief, the  $\beta$ -SiC(100)- $c(4 \times 2)$  surface structure differs significantly from the Si(100)- $c(4 \times 2)$  reconstruction.

The experiments are performed at Laboratoire de Photophysique Moléculaire, Université de Paris-Sud/Orsay using an Omicron STM at working pressures better than  $5 \times 10^{-11}$  torr. We use single crystal, single domain  $\beta$ -SiC thin films (1  $\mu\text{m}$  thick) prepared by  $\text{C}_3\text{H}_8$  and  $\text{SiH}_4$  chemical vapor deposition (CVD) growth on vicinal ( $4^\circ$ ) Si(100) wafers.  $\beta$ -SiC(100)- $c(4 \times 2)$  surfaces are routinely obtained by annealing clean and well-ordered  $\beta$ -SiC(100) $3 \times 2$  surfaces at  $1150^\circ\text{C}$  [9]. This method achieves very reproducible and clean surfaces as evidenced by sharp  $c(4 \times 2)$  LEED patterns and independently, by specific spectral features in photoemission using synchrotron radiation [3,5]. All images are very reproducible and not tip dependent and recorded at room temperature by

tunneling from the filled surface electronic states. Because of the  $\beta$ -SiC large band gap (2.3 eV), rather large bias ( $>2$  V) are needed. Unlike the  $\beta$ -SiC(100) $3 \times 2$  surface, which exhibits high-quality STM images for both filled and empty states [9], we are not able to obtain similar empty state STM images for the  $c(4 \times 2)$  reconstruction. Even at sample to tip bias up to +6 V, the empty electronic states probed by scanning tunneling spectroscopy show a flat response.

We first look at a large  $400 \times 400 \text{ \AA}$  topograph of the  $\beta$ -SiC(100) surface (Fig. 1). The surface exhibits two flat large terraces having a long range order. The main STM features are circular spots having a centered pseudo-hexagonal arrangement. The height between terraces is about  $2.3 \text{ \AA}$ , corresponding to a double height atomic step in agreement with single domain surface, as observed for  $\beta$ -SiC(100) $3 \times 2$  and Si(100) $2 \times 1$  [9,10]. Also of special interest, one can see that, in contrast to previous belief, the  $\beta$ -SiC(100)- $c(4 \times 2)$  surface is flat and of good quality, comparable to the corresponding Si(100)- $c(4 \times 2)$  surface [11]. In fact, due to very large mismatch (20%) between Si and  $\beta$ -SiC lattice parameters and CVD growth method,  $\beta$ -SiC is expected to have a large defect density. Apparently, the preparation method used here seems to reduce significantly their number.

To get the necessary insight into the surface structure, we look at the more detailed  $200 \times 200 \text{ \AA}$  topograph showing best the centered hexagon structure [Fig. 2(a)]. A close inspection of the distances between spots forming centered hexagons shows that they are not consistent with a "true" hexagonal arrangement. A zoom picture of such "pseudo-hexagons" is given in Fig. 2(b). In agreement with a centered  $(4 \times 2)$  surface ordering, the measured electronic distances between two spots along the  $XX'$  and  $YY'$

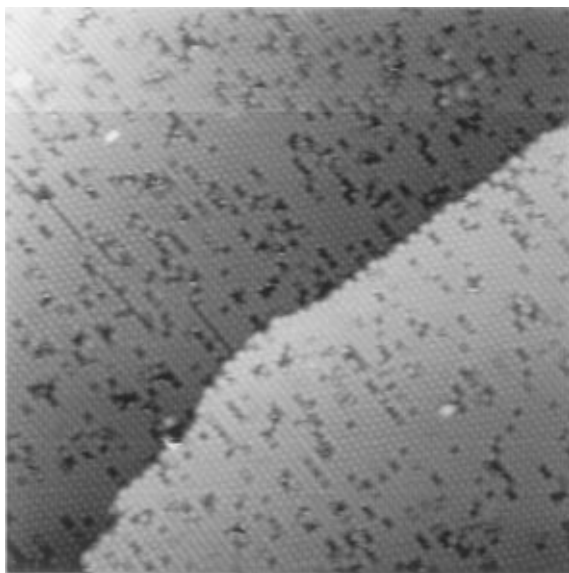


FIG. 1.  $\beta$ -SiC(100)- $c(4 \times 2)$  surface  $400 \text{ \AA} \times 400 \text{ \AA}$  STM topograph (filled electronic states). The sample bias was  $V_s = -3$  V with a 0.2 nA tunneling current.

axes are about  $x = 11.40 \text{ \AA}$  and  $y = 6.16 \text{ \AA}$ , very close respectively, to  $4 \times a$  and  $2 \times a$ , "a" being the primitive unit cell lattice parameter ( $3.08 \text{ \AA}$ ) of the nonreconstructed  $\beta$ -SiC(100) surface. Also, we can see areas [marks A, Fig. 2(a)] showing a much smaller corrugation with circular spots almost unresolved within a row. Interestingly, such regions are primarily located near higher defect density areas and give a  $2 \times 1$ -like periodicity.

Let us first emphasize that the  $c(4 \times 2)$  reconstruction model of anticorrelated asymmetric dimer surface established for Si(100) [11] is not suitable for the  $\beta$ -SiC(100)- $c(4 \times 2)$  surface. In fact, the Si(100)- $c(4 \times 2)$  STM topographs exhibit a honeycomb pattern [11] unlike our observation (Figs. 1 and 2) of centered pseudo-hexagonal patterns for the  $c(4 \times 2)$ - $\beta$ -SiC(100) surface reconstruction.

In order to get deeper insights into  $\beta$ -SiC(100)- $c(4 \times 2)$  surface structure, we plot height profiles along the  $XX'$  and  $YY'$  [Fig. 3(a)] axes that are of special interest. For the  $XX'$  axis, the profile clearly exhibits two protuberances, a dominant one corresponding to spots clearly visible on the topograph and a smaller one

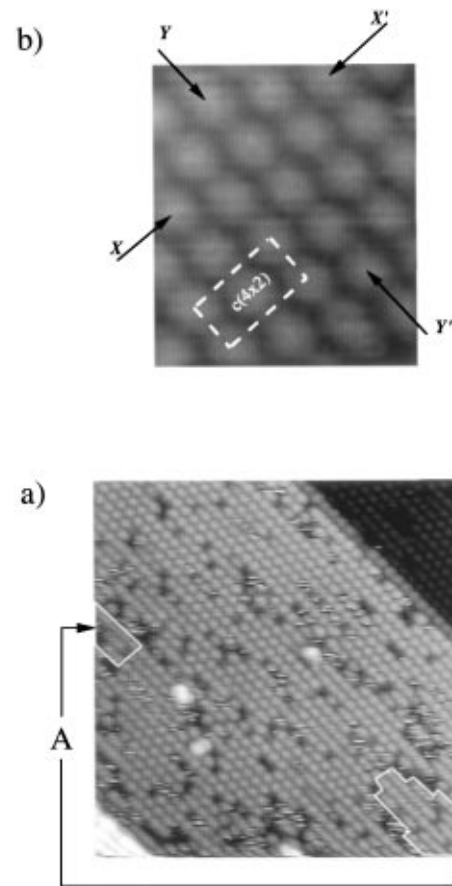


FIG. 2. (a)  $\beta$ -SiC(100)- $c(4 \times 2)$  surface  $200 \text{ \AA} \times 200 \text{ \AA}$  STM topograph (filled electronic states). Examples of area having lower corrugations are labeled A. The sample bias was  $V_s = -3$  V with a 0.2 nA tunneling current. (b) Details of an area showing the pseudo-hexagonal dimer array and the  $c(4 \times 2)$  unit cell.

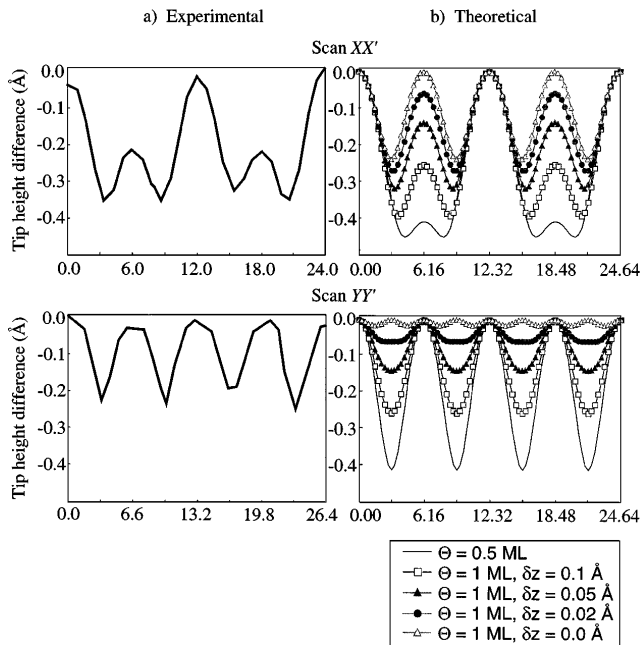


FIG. 3. (a) Experimental height profiles along  $XX'$  (top) showing two components corresponding to up and down dimers, and  $YY'$  (bottom) axis showing the component corresponding to up dimers. (b) Theoretical height profiles for various up/down dimer height differences along  $XX'$  (top) and  $YY'$  (bottom) axes calculated in a constant current mode ( $I = 0.2$  nA) at the top of the  $\beta$ -SiC(100) valence band.

indicating the presence of similar features between two of these spots. These up and down structures are separated by  $2 \times a$  along  $XX'$ . In contrast, a similar profile along the  $YY'$  axis shows no such intermediate feature between two spots.

We now have to identify the origin of the circular spots (Figs. 1 and 2), which are the major STM features. First, one should remember that the  $\beta$ -SiC(100)- $c(4 \times 2)$  surface is Si terminated with a one monolayer (1 ML) Si coverage [2–4]. The STM spots are too large to represent the print of a single Si atom, which would correspond to a very low surface coverage of  $\frac{1}{4}$  ML, far from the expected 1 ML [2,4]. Such spot shape and size have been reported to account for a Si-Si dimer on the Si(100) $2 \times 1$  surface [12]. A similar origin is, therefore, likely here with spots assigned to Si dimers giving a  $\frac{1}{2}$  ML coverage only. However, the  $XX'$  axis height profile [Fig. 3(a)] exhibits additional components between “dimers” suggesting additional dimers having a different print in the STM image and located at a lower level between “up dimers.” This gives a model in which the  $c(4 \times 2)$ - $\beta$ -SiC(100) surface reconstruction includes Si-Si dimers that are alternatively up and down within a row ( $YY'$  axis). Additional support for a model of AUDD forming such rows could be found by looking at areas A (Fig. 2). The corrugation along these rows deteriorates in some areas of higher defect density (most common defects correspond to missing dimers) locally producing a

$2 \times 1$ -like surface cell. This feature likely results from local disruption of the AUDD arrangement leading to have all dimers at the same height. This further implies the presence of down dimers.

In order to explore further such a model, we perform theoretical image calculations using the STM elastic-scattering quantum chemistry (STM-ESQC) method described in details elsewhere [13]. The bulk substrate and the tip body are both modeled by a four layer semi-infinite repetition of a SiC(100) unit cell. Lateral cyclic boundary conditions are used to avoid any distortion in the bulk band structures. In most of the present calculations, the unit cell includes eight atoms per layer. Only one Si atom forms the tip, since the experimental tips are sharp, atomlike ended, and, generally, terminated by a Si atom coming from the surface. The total valence electronic structure is taken into account for Si (3s and 3p orbitals) and for C (2s and 2p orbitals), with extended Hückel parameters [14]. We use calculated atomic positions with a 2.73 Å Si-Si dimer length and a 1.08 Å dimer-surface distance [7], the down dimer being the only one allowed to relax. We calculate constant current height profiles along the  $XX'$  and  $YY'$  axes [Fig. 3(b)] for various up dimer, down dimer height differences at  $\Theta = 1$  ML (also at  $\Theta = \frac{1}{2}$  ML for missing down dimers). Comparison with experimental scans shows that the best agreement for both  $XX'$  and  $YY'$  axes is reached for a height difference of  $\delta z = 0.1$  Å [Figs. 3(a) and 3(b)]. The calculated constant current STM image for the later case is displayed in Fig. 4(a) and compared to the experimental topograph in Fig. 4(c). As can be seen, the agreement is excellent. White circular spots in a pseudohexagonal  $c(4 \times 2)$  array are clearly visible, just as the dark gray neck located between the circular spots along the dimer rows and appearing in the  $XX'$  profile as the smaller “bump.” With missing down dimers ( $\Theta = \frac{1}{2}$  ML), the calculated image has the experimental  $c(4 \times 2)$  geometry, but this low protuberance [Fig. 3(b)] has a calculated height which is too small (0.05 Å) to account for the experimental  $XX'$  profile [Fig. 3(a)]. Anyway, a  $\frac{1}{2}$  ML coverage giving such a “neck” in the calculated STM image by orbital overlap is not consistent with experimental evidence of  $\Theta = 1$  ML [2,4]. Finally, our calculations indicate that the down dimer remains hidden to the STM tip if it has relax by more than 0.1 Å below the up dimer.

Our present results support a picture in which Si-terminated  $\beta$ -SiC(100) undergoes a  $c(4 \times 2)$  surface reconstruction at least when a flat surface having a low density of defects is prepared. A model in which Si dimers are found to form rows having alternatively up and down dimers within a row (AUDD model) account for the STM topographs. The smaller Si-Si distances for  $\beta$ -SiC ( $-20\%$  when compare to Si) is very likely to be the driving force in the formation of  $c(4 \times 2)$  surface reconstruction. As a result, the AUDD arrangement tends to reduce the surface stress by relaxing dimers up and down. The proposed model is presented in Fig. 4(b),

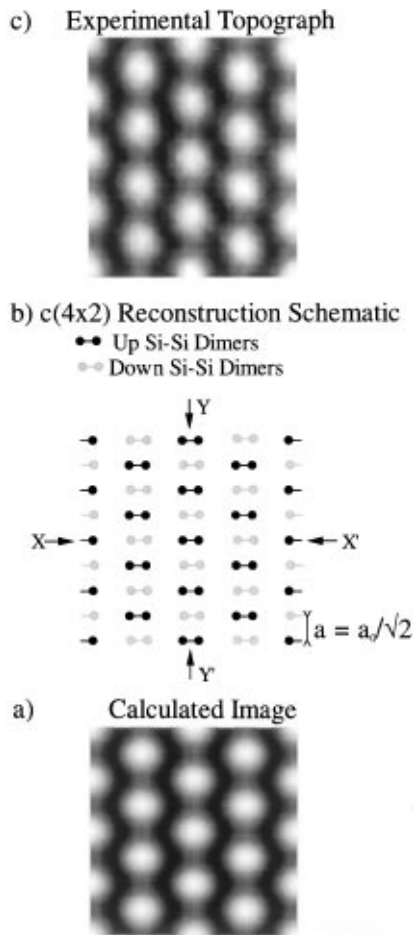


FIG. 4. (a) Calculated STM image [same conditions as in Fig. 3(b)] for a coverage  $\Theta = 1$  ML and up and down dimers separated by  $0.1 \text{ \AA}$ . The corrugation is  $0.27 \text{ \AA}$  from black to white. (b) Schematic of the  $\beta$ -SiC(100)- $c(4 \times 2)$  surface showing the alternating up and down dimers. The nonreconstructed surface primitive lattice parameter is  $a = a_0/\sqrt{2}$ , where  $a_0 = 4.36 \text{ \AA}$  is the  $\beta$ -SiC lattice constant. (c) Experimental STM topograph. For the sake of comparison with the calculated STM image [Fig. 4(a)], the contrast has been enhanced and the picture rotated by  $42^\circ$ .

which shows up and down dimers, the latter ones remaining hidden to the STM tip. One should remark that the situation observed here for the  $\beta$ -SiC(100)- $c(4 \times 2)$  surface is very different from the behavior of elemental semiconductors as Si(100)- $c(4 \times 2)$  surface, where the  $c(4 \times 2)$  reconstruction occurs only at low temperatures and results in anticorrelated asymmetric dimer rows [11]. As mentioned previously, the existence and occurrence of the  $\beta$ -SiC(100)- $c(4 \times 2)$  surface reconstruction are difficult to detect by LEED and could be inhibited by surface roughness and/or contamination [2]. Here we routinely observe the  $c(4 \times 2)$  surface reconstruction by STM. Areas with higher defect densities leaving few  $2 \times 1$ -like domains indicate that the  $2 \times 1$   $\beta$ -SiC(100) surface reconstruction seems to be driven by defects. The latter would compensate the surface stress, allowing

the down dimer to come in the same plane as the up dimer. It suggests that the  $2 \times 1$  surface arrangement probably results from a failed  $c(4 \times 2)$  reconstruction, which could be correlated to recent *ab initio* calculations questioning the existence of the  $\beta$ -SiC(100)- $2 \times 1$  surface reconstruction [7].

In conclusion, we bring the first direct observation of a  $\beta$ -SiC(100)- $c(4 \times 2)$  surface reconstruction. The STM topographs are in excellent agreement with corresponding STM image calculations. The results suggest a model of dimer rows having alternatively up and down dimers (AUDD) within the row in an “undulating” type of arrangement tending to reduce the surface stress. The  $\beta$ -SiC(100)- $c(4 \times 2)$  structure is very different from the well-known Si(100)- $c(4 \times 2)$  reconstruction. This work brings novel and deep insights into the basic knowledge of fundamentally and technologically important silicon carbide surface atomic structure.

The authors are grateful to C. Jaussaud and L. di Cioccio at LETI (CEA-Technologies Avancées) for providing  $\beta$ -SiC(100) samples and GDR 1145 “NANOMIPS” (CNRS) for support.

- [1] R.F. Davis, J. Vac. Sci. Technol. A **11**, 829 (1993); P. A. Ivanov and V.E. Chelnokov, Semicond. **29**, 1003 (1995).
- [2] R. Kaplan and V.M. Bermudez, in *Properties of Silicon Carbide*, edited by G. Harris EMIS Datareview series (INSPEC, London, 1995), Vol. 13, p. 101.
- [3] V. M. Bermudez and J.P. Long, Appl. Phys. Lett. **66**, 475 (1995).
- [4] S. Hara, W.F.J. Slijkerman, J.F. van der Veen, I. Ohdomari, S. Misawa, E. Sakuma, and S. Yoshida, Surf. Sci. Lett. **231**, L196 (1990).
- [5] M.L. Shek, Surf. Sci. **349**, 317 (1996); F. Semond, Ph.D. thesis, Université de Paris-Sud/Orsay, 1996.
- [6] J.P. Long, V.M. Bermudez, and D.E. Ramaker, Phys. Rev. Lett. **76**, 991 (1996).
- [7] M. Sabisch, P. Krüger, A. Mazur, M. Rohlfing, and J. Pollmann, Phys. Rev. B **53**, 13 121 (1996).
- [8] F. Semond, L. Douillard, P. Soukiassian, D. Dunham, F. Amy, and S. Rivillon, Appl. Phys. Lett. **68**, 2144 (1996); F. Semond, P. Soukiassian, P.S. Mangat, and L. di Cioccio, J. Vac. Sci. Technol. B **13**, 1591 (1995); M. Riehl-Chudoba, P. Soukiassian, C. Jaussaud, and S. Dupont, Phys. Rev. B **51**, 14 300 (1995).
- [9] F. Semond, P. Soukiassian, A. Mayne, G. Dujardin, L. Douillard, and C. Jaussaud, Phys. Rev. Lett. **77**, 2013 (1996).
- [10] P.E. Wierenga, J.A. Kubby, and J.E. Griffith, Phys. Rev. Lett. **59**, 2169 (1987).
- [11] R. A. Wolkow, Phys. Rev. Lett. **68**, 2636 (1992).
- [12] P. Bedrossian, Phys. Rev. Lett. **74**, 3648 (1995).
- [13] P. Sautet and C. Joachim, Chem. Phys. Lett. **185**, 23 (1991).
- [14] K. Nath and A.B. Anderson, Phys. Rev. B **41**, 5652 (1990).